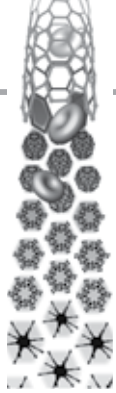

In vivo degradation of functionalized carbon nanotubes after stereotactic administration in the brain cortex

Aim: Carbon nanotubes (CNTs) are increasingly being utilized in neurological applications as components of implants, electrodes or as delivery vehicles. Any application that involves implantation or injection of CNTs into the CNS needs to address the distribution and fate of the material following interaction and residence within the neuronal tissue. Here we report a preliminary study investigating the fate and structural integrity of amino-functionalized CNTs following stereotactic administration in the brain cortex. **Materials & methods:** The CNTs investigated had previously shown the capacity to internalize in various cell types of the CNS. An aqueous suspension of multiwalled CNT-NH_3^+ was stereotactically injected into the mouse brain cortex. Their interaction with neural cells and consequent effects on the CNT structural integrity was investigated by optical, transmission electron microscopy and Raman spectroscopy of brain tissue sections for a period between 2 and 14 days post cortical administration. **Results & discussion:** The occurrence of severe nanotube structure deformation leading to partial degradation of the chemically functionalized-multiwalled CNT-NH_3^+ *in vivo* following internalization within microglia was revealed even at early time points. Such initial observations of CNT degradation within the brain tissue render further systematic investigations using high-resolution tools imperative.

Original submitted 20 October 2011; Revised submitted 19 February 2012; Published online 19 June 2012

KEYWORDS: biodegradation ■ brain ■ carbon nanomaterial ■ microglia ■ Raman spectroscopy ■ TEM

Antonio Nunes[1], Cyrill Bussy[1], Lisa Gherardini[2,3], Moreno Meneghetti[4], Maria Antonia Herrero[5], Alberto Bianco[6], Maurizio Prato[5], Tommaso Pizzorusso[2,7], Khuloud T Al-Jamal[1] & Kostas Kostarelos*[1]

[1]Nanomedicine Laboratory, Centre for Drug Delivery Research, UCL School of Pharmacy, University College London, WC1N 1AX, UK
[2]Institute of Neuroscience, Via G. Moruzzi 1, Pisa 56100, Italy
[3]CNR Institute of Clinical Physiology, Via Fiorentina 1, Siena 53100, Italy
[4]Department of Chemical Sciences, University of Padua, Via Marzolo 1, I-I-35131 Padua, Italy
[5]Department of Pharmaceutical Sciences, University of Trieste, Trieste, Italy
[6]CNRS, Institut de Biologie Moléculaire et Cellulaire, Immunologie et Chimie Thérapeutiques, 67000 Strasbourg, France
[7]Department of Psychology, University of Florence, Area San Salvi, Padiglione 26, Florence 50100, Italy
**Author for correspondence:*
Tel.: +44 207 753 5861
k.kostarelos@ucl.ac.uk

The application of nanomaterials in neuroscience is still at the early stages of development, despite an impressive body of research that is emerging [1]. Carbon-based nanostructures, such as carbon nanotubes (CNTs), are some of the most interesting types of novel materials proposed for the design of nanomaterial-based neurological interventions [2]. Although as-produced CNTs are insoluble in most aqueous solvents, the development of functionalization chemistries for their surface has led to a notable enhancement in aqueous dispersibility, which has allowed for their application in physiological environments, including the CNS [3]. The scope of their biological applications [4] has broadened dramatically in the last few years, ranging from therapeutics and diagnostics for oncology [5], to neuroprosthetic devices [6].

The interactions, binding and internalization of different types of CNTs into a variety of tissues *in vitro* and *in vivo* is imperative [7]. The role of functionalized-CNT characteristics, such as surface charge density or length on interaction with cells and tissues, is under investigation both in relation to biological mechanisms and toxicological responses [8]. However, knowledge regarding their fate following cellular internalization within the CNS tissue remains scarce. Understanding the prevailing interactions between CNTs and neural cells *in vivo*, along with their internalization mechanism, intracellular translocation and subcellular localization is of major importance, particularly in view of their potential as drug or gene delivery vectors. Lee *et al.* have recently shown that amine-functionalized single-walled CNTs (SWCNTs) injected directly in the ventricles were able to exert activity against inflammation and protect neurons after induction of ischemic damage, even though the mechanism for such activity remains elusive [9]. More recently, we have shown that functionalized-multiwalled CNTs (*f*-MWCNTs) (amine-functionalized by the 1,3-dipolar cycloaddition reaction) were able to efficiently deliver siRNA to neurons, leading to enhanced cell survival by silencing Caspase 3 and resulting in significant recovery of ischemia-induced motor cortex function [10].

Any approach that involves implantation or injection of CNTs into the CNS will need to determine the fate of the nanomaterial following interaction with neuronal tissue. In this study, and in continuation from our recently published work [10], a suspension of the chemically same *f*-MWCNTs (MWCNT-NH_3^+)

were stereotactically injected into the mouse brain cortex in the absence of any therapeutic agent, and their interaction with neural cells was investigated by transmission electron microscopy (TEM) and Raman spectroscopy of brain tissue sections. The aim of this study was to investigate the fate of *f*-MWCNTs with a proven capacity to be effective vectors for the delivery of siRNA in the brain, within neuronal tissue *in vivo*, during the time frame of 2 days and 2 weeks after cortical administration.

Materials & methods

Materials

MWCNTs were purchased from Nanostructured and Amorphous Materials Inc. (TX, USA; Lot #1240XH, 95%). The outer average diameter was 20–30 nm, and the length was 0.5–2 µm. The chemicals and solvents were obtained from Sigma-Aldrich (MO, USA) and were used as received. The 400-mesh copper grids coated with formvar/carbon support film for TEM were purchased from Agar Scientific (Essex, UK). The Euthatal® was obtained from Rhone Merieux (Harlow, UK).

Chemical functionalization & characterization of CNTs

1,3-dipolar cycloaddition reaction on purified MWCNTs was followed as described in [3]. MWCNTs (100 mg) were suspended in 150 ml of dimethylformamide solution. The mixture was sonicated and then heated at 115°C while a solution of paraformaldehyde (4 × 100 mg) and *tert*-butyloxycarbonyl monoprotected 2,2'-(ethylenedioxy) diethylamine (4 × 100 mg) in dimethylformamide solution were added by portions over 4 days. The product was filtrated, washed with dimethylformamide solution, MeOH and ether, and the black solid was dried. The amino acid was then deprotected with HCl gas and the obtained MWCNT-NH_3^+ was thoroughly washed and dried. The amount of amino groups was determined with the Kaiser test, corresponding to 147 µmol/g. TEM characterization showed that the morphology of the nanotubes was not modified by the 1,3-dipolar cycloaddition. The tubes were also characterized by thermogravimetric analysis as shown previously [10].

TEM micrograph of *f*-MWCNT aqueous dispersions

f-MWCNT powder was hydrated in 5% dextrose at 1 mg/ml concentration, by bath-sonicating the dispersions for 15–30 min. The sonicated *f*-MWCNT dispersions were deposited on 400-mesh copper grids coated with formvar/carbon support film and allowed to dry at room temperature before imaging under TEM (Philips CM10). The images were captured with a high-resolution digital camera coupled to the microscope. High-resolution TEM images were captured using an FEI T20 transmission electron microscope.

Animal handling & experimentation

All animal experiments were performed in compliance with the UK Home Office (1989) Code of Practice for the Housing and Care of Animals Used in Scientific Procedures and in agreement with protocols approved by the Italian Ministry for Scientific Research. The 6–8-week-old C57BL/6 females were caged in groups of four to seven, with free access to food and water. A temperature of 19–22°C was maintained, with a relative humidity of 45–65%, and a 12-h light/dark cycle. To perform these experiments, three mice per group per time point were used.

Stereotactic administration of *f*-MWCNTs

C57BL/6 mice were anesthetized with Avertin® (0.5 ml/100 g; Acros Organics, Gell, Belgium) and mounted on a stereotactic apparatus. Injections of up to 1 µl volume were made at specific stereotactic locations (Bregma +0.5 and +1.5 mm from sagittal line) in the motor cortex by means of a glass pipette (30 µm tip diameter) mounted on a motorized (0.1 µm step) three-axis micromanipulator connected to an injector (Sutter Instruments, CA, USA). A total of 1 µl of CNT dispersion was released at 700 µm below the cortical surface. During injections, the animals were oxygenated and heated using a blanket with a thermostat to ensure a 37°C body temperature. At the end of all surgical procedures, the scalp incision was closed with Mersilk sutures (Ethicon, Scotland, UK), and the antibiotic, gentamicin, was topically administered to prevent infections. In these conditions the whole procedure required approximately 20 min, and recovery from anesthesia occurred after 60–90 min. After recovery, the animals were returned to their home cages. Mice were culled at 2 and 14 day time points.

Brain tissue sectioning & TEM

Mice were transcardially perfused under terminal anesthesia (Euthatal) with 3% glutaraldehyde in 0.5 M cacodylate buffer (pH 7.4). After perfusion, brains were removed,

immersed in the perfusate for 2–4 days at 4°C, allowing adequate penetration of the primary fixative. The brains were then transferred to the 1 M cacodylate buffer until they were ready for processing. Just before embedding, brain coronal sections of 1 mm were prepared using a mouse brain matrix (Zivic Instruments®, PA, USA). Coronal sections that contained the cortical region injected with either *f*-MWCNTs or vehicle were then washed several times with deionized water, submitted to a second fixation with OsO_4 for 90 min, rinsed with deionized water, and then dehydrated by a series of ethanol grades: 70, 90 and 100%. Brain specimens were infiltrated with propylene oxide, followed by 1:1 (v/v) propylene oxide:araldite resin and were finally left in neat resin overnight at room temperature. Brain coronal sections were then placed at the desired orientation in the embedding moulds and placed in a 60°C oven to allow for resin polymerization for 2–3 days. A small region of the coronal section in the close vicinity of the cortical site of injection (2 × 2 mm) was then selected for semithin sectioning. Semithin sections (~0.71-µm thickness) were prepared using an ultramicrotome equipped with SEMi diamond knife (SEMi, Leica Microsystems, Peterborough, UK), and then stained with toluene blue to be observed under a light microscope: ultrathin sectioning was performed in regions where CNT presence was apparent. TEM imaging was performed on precisely aligned ultrathin sections (~70-nm thickness) obtained by an ultramicotome and a diamond knife (Diatome 45°, Leica Microsystems). The sections were collected onto 400-mesh copper 3.05-mm grids (Athene grids, Agar Scientific) and observed under TEM without further negative staining.

Brain tissue sectioning & Raman spectroscopy

Mice brains for Raman analysis were removed, snap frozen by immersion into isopentane, precooled in liquid nitrogen, and then stored at -80°C until further analysis. Sections with a 20-µm thickness were prepared on a cryomicrotome (Leica Microsystems; CM3050S), air-dried for 1 h at room temperature, postfixed in methanol, precooled at -20°C, and then left to dry and kept at room temperature before analysis. Raman spectra were recorded on a Renishaw inVia microRaman equipped with a Leica microscope and a He–Ne laser (633 nm), using a 50× objective lens at 5% of the total laser power. Raman scattering signals were acquired on brain regions where black material appeared. Raman spectra were corrected for tissue auto-fluorescence and normalized to G band intensity.

Results & discussion

The physical and morphological characteristics of the MWCNT-NH_3^+ material used in this study were recently published [10]. Briefly, the degree of ammonium functional groups grafted on the *f*-MWCNTs was 147 µmol/g of material and their length distribution was between 0.5 and 2 µm, with a diameter in the range of 20–30 nm. TEM analysis showed that MWCNT-NH_3^+ were largely debundled and generally appeared as individualized nanotube dispersions (Figure 1A).

Internalization of nanotubes into cultured microglia and neurons has been reported previously in [11,12]; however, no study has interrogated the determinant factors of such interactions. In this study, MWCNT-NH_3^+ (0.5 µg/mouse) were stereotactically injected at specific coordinates in the motor cortex of a mouse brain (Figure 1B) and, 2 days postinjection, ultrathin sections of brain parenchyma near the injection site were prepared for TEM examination (Figure 2). In order to improve visualization of *f*-MWCNT at the cellular level, TEM imaging was performed on unstained sections. Microscopic analysis of tissue sections 2 days postadministration suggested that MWCNT-NH_3^+ were dispersed and spread in the vicinity of the injection site and the brain parenchyma. It also confirmed their ability to internalize within different types of brain cells (Figure 2A & 2B), including both microglia and neurons. Microglial internalization of nanotubes was widespread and seems to be the predominant mechanism of early-time tissue response. This observation also agreed with previous reports following intratumoral injection of nanotubes within a brain-implanted glioblastoma model [13,14], despite the inherent differences in tissue architecture and levels of pre-existing microglial activation between normal brain and the glioblastoma mass.

The widespread internalization of MWCNT-NH_3^+ by microglia is shown in Figure 2C–2H. Higher magnification in the cytoplasmic region of the cells containing nanotubes indicated that when in clusters or aggregates, the material is localized in vesicular structures (presumably phagolysosomal vesicles). At the same time, individual nanotubes were

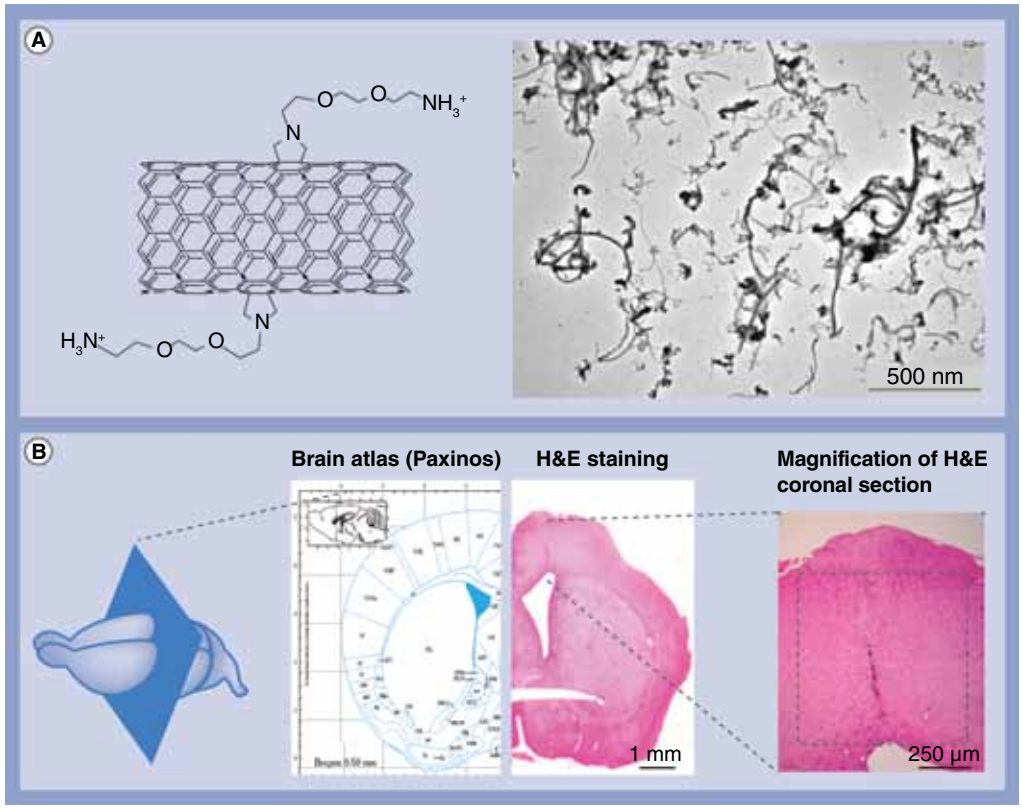

Figure 1. Stereotactic administration of chemically functionalized-multiwalled carbon nanotubes in the motor cortex of mice. (A) Chemically functionalized-multiwalled carbon nanotubes (MWCNT-NH_3^+) used in the experiment: chemical structure and transmission electron microscope (TEM) image of MWCNT-NH_3^+ dispersed in 5% dextrose at 250 µg/ml final concentration. **(B)** Coordinates of the stereotactic injection. MWCNT-NH_3^+ were injected at specific coordinates into the M1/M2 brain regions of the mouse motor cortex (according to [24]): latero–lateral (*x*) +0.5 mm, dorso–ventral (*y*) +1.5 mm, rostro–caudal (*z*) 0.7 mm. At 2 days postinjection, brains were isolated and coronal sections were processed for H&E staining and TEM imaging. The area surrounded by a dashed square (1 mm^2) represents the area processed further for TEM analysis. H&E: Hematoxylin and eosin.

also found either in the cytoplasm or crossing the vesicular membranes after internalization (arrows in Figure 2D). Mu *et al.* proposed a working hypothesis for the determination of the crucial parameters and factors affecting *in vitro* cellular uptake of chemically functionalized CNTs, suggesting that aggregates of carboxylated MWCNTs or ammonium MWCNTs were mainly internalized via active endocytosis (or phagocytosis – dependent on cell type and dimensions of the material interacting with the cells), whereas individualized ammonium MWCNTs could enter the cells through a direct membrane translocation pathway [15]. We also recently reported data in agreement with such a hypothesis using nonphagocytic A549 cells and primary human monocyte-derived macrophages, a professional phagocytic cell type [16]. In these studies, the direct translocation of MWCNT-NH_3^+ was confirmed by high-resolution 3D electron microscopy, by piercing the plasma membrane on nanotube entrance into cells or after vesicular internalization by piercing the vesicular membrane to escape into the cytoplasm [16]. In both cases, individualization of nanotubes facilitated the process. In the present study, similar observations were obtained *in vivo* after direct injection of MWCNT-NH_3^+ in the cortex parenchyma.

Based on the same TEM analysis of the brain tissue sections, 2 days postinjection, it was observed that within many microglia, which internalized MWCNT-NH_3^+, large clusters of seemingly decomposed nanotube material existed (Figure 2F & 2H). Intrigued by such observations, we decided to further investigate the morphology of these structurally undefined materials that could be found within the cytoplasm of many cells throughout the brain sections. Most nanotubes that localized intracellularly were seen intact; however,

widespread structural changes were also evident, suggesting the initiation of a degradation process. As can be seen in FIGURE 3, numerous areas contained nanomaterial debris that had suffered severe structural deformations, reduced length and loss of cylindrical structure (FIGURE 3A–3C). Higher magnification at the interface of such clusters indicated the presence of both intact and structurally deformed MWCNT-NH_3^+ in the cytoplasm of microglial cells *in vivo*. Moreover, FIGURE 3C offered further insight as to how this degradative process may be evolving, with the co-existence of intact CNT structures (FIGURE 3C, II), carbon sheets that seem unraveled from the concentric cylindrical conformation (FIGURE 3C, III) and also the decomposed material that had clearly lost all structural features resembling a nanotube (FIGURE 3C, IV).

In order to further investigate these structural observations using a macroscopic technique, and also to interrogate the pristine nature of the graphitic material localized intracellularly, we performed Raman spectroscopy of the brain coronal sections (FIGURE 4). Animals were injected with MWCNT-NH_3^+ stereotactically at the same cortical location and brain tissue was removed after 2 and 14 days postinjection for sectioning. FIGURE 4A shows how optical

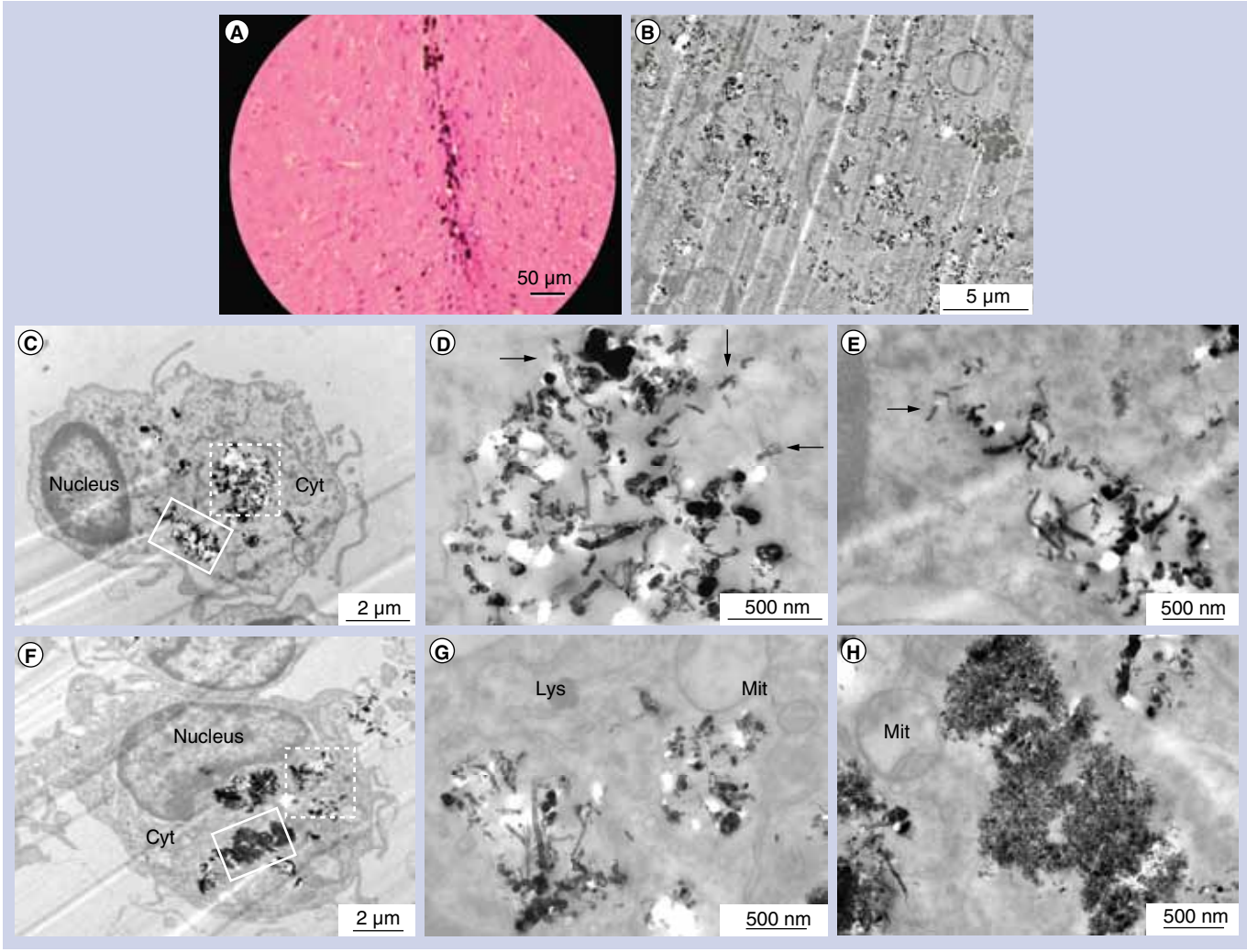

Figure 2. Uptake of chemically functionalized-multiwalled carbon nanotubes by microglia *in vivo*. (A) High magnification of hematoxylin and eosin-stained coronal section, representative of the area processed for transmission electron microscopy analysis. Chemically functionalized-multiwalled carbon nanotubes (MWCNT-NH_3^+) were mainly detected in an area of approximately 225 µm × 225 µm (50 nm^2) around the injection site. **(B)** Transmission electron microscopy of brain parenchyma close to the injection site. **(C)** Low magnification image of microglia with MWCNT-NH_3^+ localized intracellularly. **(D)** High magnification of the dashed box in **(C)**, showing individualized MWCNT-NH_3^+ enclosed within an intracellular vesicular membrane. **(E)** High magnification of the solid box in **(C)**, showing individualized MWCNT-NH_3^+ that are free in the cytoplasm. **(F)** Low magnification image of other microglia showing MWCNT-NH_3^+ localized intracellularly, exhibiting the co-existence of individualized and intact MWCNT-NH_3^+ nanotube debris. **(G)** High magnification of the dashed box in **(F)**. High magnification of the solid box in **(F)**.
Cyt: Cytoplasm; Lys: Lysosome; Mit: Mitochondria.

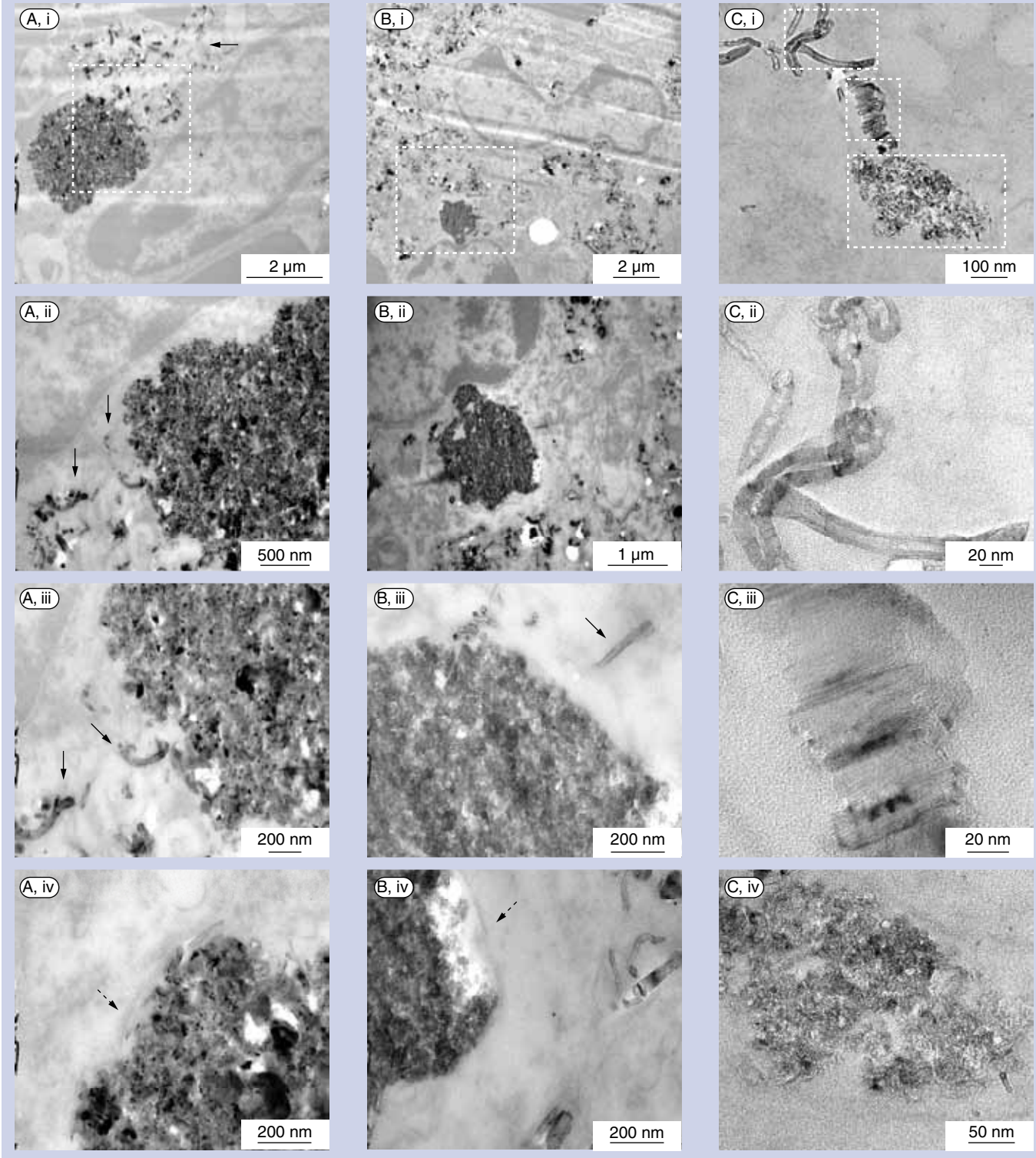

Figure 3. Evidence of degradation of chemically functionalized-multiwalled carbon nanotubes residing within microglia *in vivo*. Intracellular chemically functionalized-multiwalled carbon nanotubes (MWCNT-NH_3^+) imaged with severe structural deformations, reduced length and loss of cylindrical structure by transmission electron microscopy. **(A, i & B, i)** Low magnification micrographs showing different microglial cells containing MWCNT-NH_3^+ in their cytoplasm. **(A, ii & B, ii)** High magnification micrographs of dashed boxes in **(A,i)** and **(B, i)**, respectively. **(A, iii & B, iii)** High magnification micrographs showing examples of MWCNT-NH_3^+ that lost their cylindrical shape. Intact tubular structured nanotubes (solid arrow) can also be detected in the periphery of these clusters. **(A, iv & B, iv)** High magnification micrographs of panels **(A, i)** and **(B, i)**, respectively, showing nanotubes with signs of morphological change presumably enclosed within an intracellular vesicle (dashed arrows point to the membranous boundary). **(C, i & C, ii)** High-resolution micrographs with co-existing individualized, intact MWCNT-NH_3^+; **(C, iii)** carbon sheets unraveling their concentric cylindrical conformation and; **(C, iv)** degraded nanotube material with almost complete loss of their structural integrity.

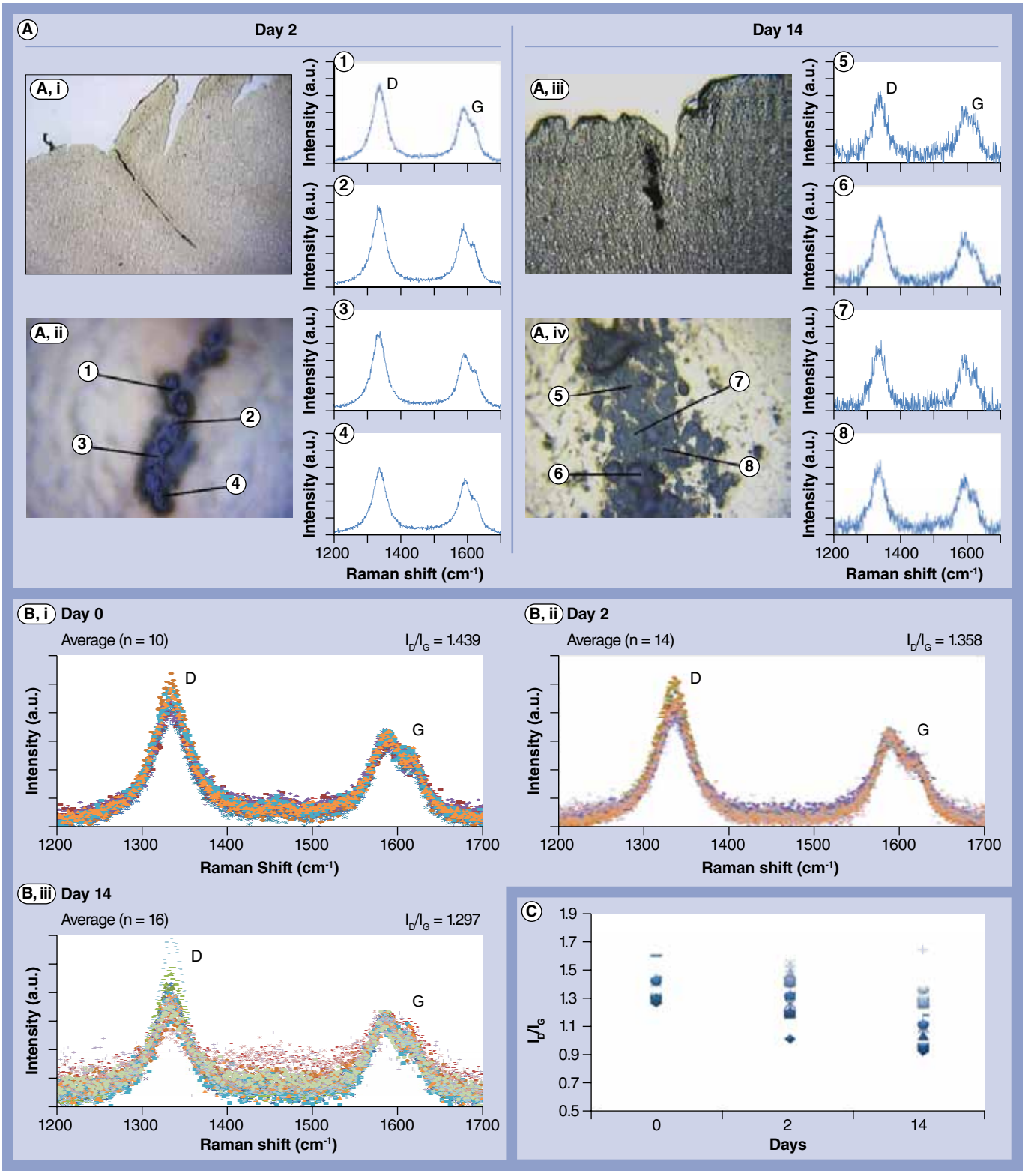

Figure 4. Raman spectroscopy of brain tissue sections 2 and 14 days after stereotactic administration of chemically functionalized-multiwalled carbon nanotubes. (A) Raman spectra of 20-µm thick brain sections, 2 days (left) and 14 days (right) postinjection. Spectra presented are representative data, corresponding to locations 1–8 **(A,ii & A,iv)** indicated in the optical microscopy images. **(B)** Collated Raman spectra as acquired from the starting material before injection (0 days) **(B, i)** and from brain sections at 2 days **(B, ii)** and 14 days postinjection **(B, iii)**. The intensity ratio between D and G bands (I_D/I_G) indicated was calculated from the average intensities of D and G bands at each time point (n = 10, n = 14 and n = 16 spectra used for each time point, respectively). Average intensity of G band was normalized to 1. **(C)** I_D/I_G band ratio calculated from Raman spectra in each region of interest in the section. An overall reduction in I_D/I_G ratio was observed with time, suggesting dramatic changes in the carbon structure of the nanotubes inside the brain. I_D/I_G: Intensity ratio between D and G bands.

microscopy of the tissue sections at the injection site was used to obtain the Raman spectral analysis at different locations. Typical Raman spectra were obtained at different regions of the brain sections, 2 and 14 days postinjection. While characteristic Raman spectra of MWCNT (with D and G peaks) were obtained, we observed that after 14 days the material exhibited an overall reduction in the intensity of the characteristic peaks with increased background noise, suggesting the presence of less intact CNTs (Figure 4A & 4B). The characteristic D/G band intensity ratio, which is considered an indication of the degree of structural defects, was also distorted with time (i.e., overall decrease of the ratio), suggesting severe changes in the carbon structure of the material residing in the tissue (Figure 4B & 4C).

Evidence that oxidative conditions (irrespective of pH) [17] can induce degradation of CNTs has consistently emerged since Allen *et al.* [18] first reported the biodegradation of SWCNTs after incubation with horseradish peroxidase in the presence of H_2O_2 under static conditions (at 4°C for 12 weeks) [18,19]. Kagan *et al.* also demonstrated that SWCNTs could be degraded by the catalytic action of human neutrophil myeloperoxidase and, more importantly, have shown that the degraded nanotubes did not induce an inflammatory response when aspirated into the lungs of mice [20]. Complete degradation of CNTs leading to CO_2 molecules has been reported previously and may lead to an overall naive, fully biocompatible profile of tissue-residing CNTs [18,19,21]. However, degradation of CNTs may generate molecular species rich in aromatic rings and other by-products, such as polyaromatic hydrocarbons that will have a different cytotoxic profile. In any case, the long-term biological consequences from CNT degradation should be further considered and investigated.

Recently, it has been reported that the oxidative degradation of carboxylated SWCNTs and MWCNTs in test tubes indicates that both types can undergo degradation, albeit to a different extent [22]. Likewise, Zhao *et al.* studied the enzymatic degradation of different MWCNTs (purified, oxidized and nitrogen-doped) using similar in-test-tube assays and demonstrated that MWCNT degradation greatly depended on their degree of carboxylation [21]. Liu *et al.* also studied the effect of surface functionalization on CNT degradation and showed that pristine, ozone-treated and aryl-sulfonated nanotubes could not degrade as effectively as oxidized SWCNTs under phagolysosomal-mimicking conditions [17]. These studies, independently reported by three different groups, demonstrated that degradation of different types of CNT (both SWCNTs and MWCNTs) can indeed occur [17,21,22]. Further studies are needed to systematically address the factors that will control the rate of the degradative process (e.g., enzymatic profile of host tissue and type of CNT surface functionalization).

In the context of the present study, microglia have often been associated with oxidative processes that may be related to their highly efficient capacity for phagocytosis and their role in response to even subtle neuronal injury. Microglial cells are the resident immune effectors of the CNS, and as such their oxidative lysosomal environment, with low pH and the presence of hydrolytic enzymes may further promote the degradation of the CNTs. However, this remains a working hypothesis at this stage until further evidence arises from work currently undertaken.

This study reports the occurrence of partial degradation of MWCNT-NH_3^+ *in vivo* following internalization and intracellular localization within microglia after direct stereotactic injection in the motor cortex. The degradative processes and mechanisms taking place were not elucidated in this study; however, TEM analysis of the tissue sections offered structural evidence that widespread nanotube degradation can start within 2 days postinjection. Lastly, while this study was in press, another group reported the occurrence of SWCNT degradation in the lung of animals by pharyngeal aspiration [23]. These two reports offer the first direct evidence of degradation of CNTs within two different tissues. Such initial evidence provide great impetus for further investigation to explore the critical parameters that will determine the kinetics and rate-limiting factors of CNT *in vivo* degradation. It has to be stressed that degradation of CNTs may be (e.g., drug delivery and diagnostics) or may not be desirable (e.g., implants, neuroprosthetic devices and scaffolds) depending on the intended biomedical application. If degradability of CNTs is desired, engineering material that will allow rapid and complete degradation within the tissues in which they reside will change the landscape regarding the overall toxicological profile of carbon structures that is critically dependent on tissue biopersistence.

Acknowledgements

The authors wish to acknowledge the Electron Microscope Unit at UCL Institute of Neurology, Queen Square, London, UK, for the collaboration.

Financial & competing interests disclosure

This work was supported partially by the European Union FP6 NINIVE (NMP4-CT-2006-033378) and FP7 ANTICARB (HEALTH-2007-201587) projects. M Prato acknowledges financial support from the ERC Advanced Grant (CARBONANOBRIDGE-ERC-2008-227135), Italian Ministry of Education (MIUR, Cofin Prot. 20085M27SS and FIRB prot. RBAP11ETKA) and AIRC (AIRC 5 per mille Rif. 12214). A Bianco wishes to acknowledge the Centre National de la Recherche Scientifique for financial support from PICS (Project for International Scientific Cooperation). C Bussy is a Marie-Curie Fellow under the FP7 NANONEUROHOP fellowship (REA-276051). The authors have no other relevant affiliations or financial involvement with any organization or entity with a financial interest in or financial conflict with the subject matter or materials discussed in the manuscript apart from those disclosed.

No writing assistance was utilized in the production of this manuscript.

Ethical conduct of research

The authors state that they have obtained appropriate institutional review board approval or have followed the principles outlined in the Declaration of Helsinki for all human or animal experimental investigations. In addition, for investigations involving human subjects, informed consent has been obtained from the participants involved.

Executive summary

- Stereotactic injection of chemically functionalized-multiwalled carbon nanotubes (CNTs) into mouse cortex led to uptake within microglia cells.
- Partial degradation of functionalized-multiwalled CNTs was observed as structural deformation of the nanotubes by transmission electron microscopy.
- Widespread structural changes were visible by transmission electron microscopy 2 days postinjection, suggesting early onset of a degradation process.
- Degradation of nanotubes was manifested as structural deformations, reduced length and loss of cylindrical structure.
- There was a reduction in the intensity of the Raman spectroscopy peaks and increased background noise of brain sections in the vicinity of the injection site.
- Experimental evidence that multiwalled CNT-NH_3^+ undergo dramatic structural tranformations intracellularly (within microglia) after injection in the brain.

References

Papers of special note have been highlighted as:
- ▪ of interest
- ▪▪ of considerable interest

1 Nunes A, Al-Jamal KT, Kostarelos K. Therapeutics, imaging and toxicity of nanomaterials in the central nervous system. *J. Control. Release* (2012) (In Press).

2 Nunes A, Al-Jamal K, Nakajima T, Hariz M, Kostarelos K. Application of carbon nanotubes in neurology: clinical perspectives and toxicological risks. *Arch. Toxicol.* (2012) (In Press).

▪ **Overview of the clinical perspectives using carbon nanotubes (CNTs) in neurology and the toxicological risks.**

3 Georgakilas V, Kordatos K, Prato M, Guldi DM, Holzinger M, Hirsch A. Organic functionalization of carbon nanotubes. *J. Am. Chem. Soc.* 124(5), 760–761 (2002).

4 Kostarelos K, Bianco A, Prato M. Promises, facts and challenges for carbon nanotubes in imaging and therapeutics. *Nat. Nanotechnol.* 4(10), 627–633 (2009).

5 Podesta JE, Al-Jamal KT, Herrero MA *et al.* Antitumor activity and prolonged survival by carbon-nanotube-mediated therapeutic siRNA silencing in a human lung xenograft model. *Small* 5(10), 1176–1185 (2009).

6 Keefer EW, Botterman BR, Romero MI, Rossi AF, Gross GW. Carbon nanotube coating improves neuronal recordings. *Nat. Nanotechnol.* 3(7), 434–439 (2008).

7 Kostarelos K, Lacerda L, Pastorin G *et al.* Cellular uptake of functionalized carbon nanotubes is independent of functional group and cell type. *Nat. Nanotechnol.* 2(2), 108–113 (2007).

8 Ali-Boucetta H, Al-Jamal KT, Müller KH *et al.* Cellular uptake and cytotoxic impact of chemically functionalized and polymer-coated carbon nanotubes. *Small* 7(22), 3230–3238 (2011).

9 Lee HJ, Park J, Yoon OJ *et al.* Amine-modified single-walled carbon nanotubes protect neurons from injury in a rat stroke model. *Nat. Nanotechnol.* 6(2), 121–125 (2011).

▪▪ **First study to report the application of CNTs as neuroprotective agents in stroke models.**

10 Al-Jamal KT, Gherardini L, Bardi G *et al.* Functional motor recovery from brain ischemic insult by carbon nanotube-mediated siRNA silencing. *Proc. Natl Acad. Sci. USA* 108(27), 10952–10957 (2011).

▪▪ **First study to report the use of CNTs as vectors for siRNA-gene silencing leading to functional recovery in an induced stroke model.**

11 Kateb B, Van Handel M, Zhang L, Bronikowski MJ, Manohara H, Badie B. Internalization of MWCNTs by microglia: possible application in immunotherapy of brain tumors. *Neuroimage* 37(Suppl. 1), S9–S17 (2007).

12 Cellot G, Ballerini L, Prato M, Bianco A. Neurons are able to internalize soluble carbon nanotubes: new opportunities or old risks? *Small* 6(23), 2630–2633 (2010).

13 Zhao DC, Alizadeh D, Zhang L *et al.* Carbon nanotubes enhance CpG uptake and potentiate antiglioma immunity. *Clin. Cancer Res.*17(4), 771–782 (2011).

▪ **Describes the use of CNTs as delivery vectors to potentiate CpG immunotherapy in an intracranial glioma model.**

14 VanHandal M, Alizadeh D, Zhang L *et al.* Selective uptake of multi-walled carbon nanotubes by tumor macrophages in a murine glioma model. *J. Neuroimmunol.* 208(1–2), 3–9 (2009).

15 Mu QX, Broughton DL, Yan B. Endosomal leakage and nuclear translocation of multiwalled carbon nanotubes: developing a model for cell uptake. *Nano Lett.* 9(12), 4370–4375 (2009).

16 Lacerda L, Russier J, Pastorin G *et al.* Translocation mechanisms of chemically functionalised carbon nanotubes across plasma membranes. *Biomaterials* 33(11), 3334–3343 (2012).

17 Liu X, Hurt RH, Kane AB. Biodurability of single-walled carbon nanotubes depends on surface functionalization. *Carbon NY* 48(7), 1961–1969 (2010).

18 Allen BL, Kichambare PD, Gou P *et al.* Biodegradation of single-walled carbon nanotubes through enzymatic catalysis. *Nano Lett.* 8(11), 3899–3903 (2008).

▪▪ **First study to show the possibility of degradation of CNTs under *in vitro* conditions.**

19 Allen BL, Kotchey GP, Chen Y *et al.* Mechanistic investigations of horseradish peroxidase-catalyzed degradation of single-walled carbon nanotubes. *J. Am. Chem. Soc.* 131(47), 17194–17205 (2009).

20 Kagan VE, Konduru NV, Feng W *et al.* Carbon nanotubes degraded by neutrophil myeloperoxidase induce less pulmonary inflammation. *Nat. Nanotechnol.* 5(5), 354–359 (2010).

21 Zhao Y, Allen BL, Star A. Enzymatic degradation of multiwalled carbon nanotubes. *J. Phys. Chem. A* 115(34), 9536–9544 (2011).

22 Russier J, Ménard-Moyon C, Venturelli E *et al.* Oxidative biodegradation of single- and multi-walled carbon nanotubes. *Nanoscale* 3(3), 893–896 (2011).

23 Shvedova AA, Kapralov AA, Feng WH *et al.* Impaired clearance and enhanced pulmonary inflammatory/fibrotic response to carbon nanotubes in myeloperoxidase-deficient mice. *PLoS ONE* 7(3), e30923 (2012).

24 Paxinos G, Franklin KBJ. *The Mouse Brain in Stereotaxic Coordinates (3rd Edition).* Academic Press, CA, USA, 1–360 (2008).